Mode field converter based on embedded photonic crystal fiber

Weimin Sun (孙伟民)[1*], Xiaoqi Liu (刘晓颀)[1], Quan Chai (柴 全)[1], Jianzhong Zhang (张建中)[1], Fenghua Fu (付枫华)[1], Yu Jiang (姜 宇)[1], and Tim A. Birks[2]

[1] *College of Science, Harbin Engineering University, Harbin 150001, China*

[2] *Department of Physics, University of Bath, Claverton Down, Bath BA2 7AY, UK*

[*] *E-mail: weimin_sun2003@yahoo.com.cn*

Received July 14, 2009

Six high-index cores are embedded around the central solid core of the photonic crystal fiber to form a fiber embedded photonic crystal fiber (FEPCF), which is investigated based on the beam propagation method. In this structure, the Gaussian mode could be transferred to the ring mode. So FEPCF could used as a mode convertor.

OCIS codes: 060.2280, 060.2340, 060.5295, 230.3990.

doi: 10.3788/COL20090710.0921.

Photonic crystal fibers (PCFs) were firstly fabricated in 1996 by Knight *et al.*[1], and since then, a lot of invents and applications are based on these exciting new-generation fibers. PCFs are formed of silica (or another glass) with a two-dimensional pattern of air holes running down their length[2]. The structure of PCFs could be changed by inserting some other materials into the air holes and is widely used in the pumped PCF laser. The controlled excitation of higher order modes in optical fibers has received considerable attention recently[3]. Fiber mode converter is useful in dispersion compensation[4], nonlinear application[5], and useful loss[6]. To achieve designed modes other than the fundamental mode, many techniques were developed, for LP_{02}[3,7] and LP_{11} mode converters[8]. Most reported converters were fabricated using the ferrule technique on a drawing tower or controlling the hole inflation of an existing PCF on a tapering rig. All these methods need ingenious fabrication technology and are very complex. We proposed a novel PCF structure of a central solid core, surrounded by a ring of higher-index cores, which could be fabricated based on fiber-embedded technique[9]. We expect to produce a convenient mode converter by cutting a section of the fiber-embedded photonic crystal fiber (FEPCF). To search an optimized structure of the FEPCF, we change their structure parameters and compare the mode fields and dispersion characteristics. To guarantee coupling efficiency and splicing effect, we prefer a solid central core to a central hole when we design the structure of PCF.

According to Birks's analysis[10,11], PCFs can only guide fundamental mode if the ratio of hole diameter to pitch between two holes is less than 0.42. This type of PCF is called as the endless single-mode photonic crystal fiber (ESPCF). If the central solid core is replaced by a dual-core structure, the behavior of the PCF would change dramatically. One input mode could be converted to another mode by this dual-core structure.

As a reference, we firstly analyze the mode characteristics of an ESPCF of $d = 4.4$ μm in diameter and $\Lambda = 12$ μm in pitch. Its cross-section is shown in Fig. 1(a). Because the ratio of the diameter to the pitch is less than 0.42, only the fundamental mode could be transmitted along the ESPCF with negligible loss. When the injected mode is a Gaussian one (Fig.1(b)), the light propagation could be calculated using the beam propagation method (BPM), as shown in Fig. 1(c). We compare the mode structure within the ESPCF under different wavelengths, and find that these mode fields are quite similar (Figs. 1(d) and (e)).

Without changing the air-hole cladding, we replace the central core with a dual-core to form FEPCF, as shown in Fig. 2(a). The six outer embedded cores are of higher refractive index. The diameter of the embedded

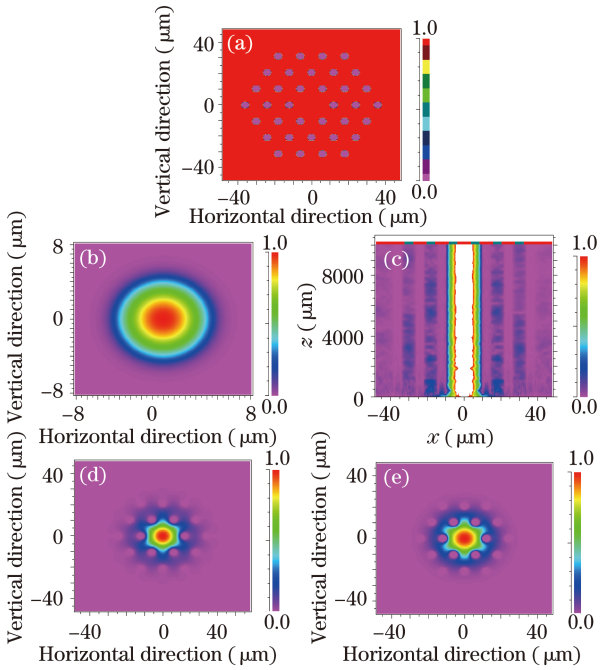

Fig. 1. Characteristics of ESPCF of $d = 4.4$ μm and $\Lambda = 12$ μm. (a) Structure of the ESPCF; (b) mode field of the input light; (c) propagation along the fiber; (d) $\lambda = 1.60$ μm, $n_{\rm eff} = 1.442423$; (e) $\lambda = 0.65$ μm, $n_{\rm eff} = 1.456334$.

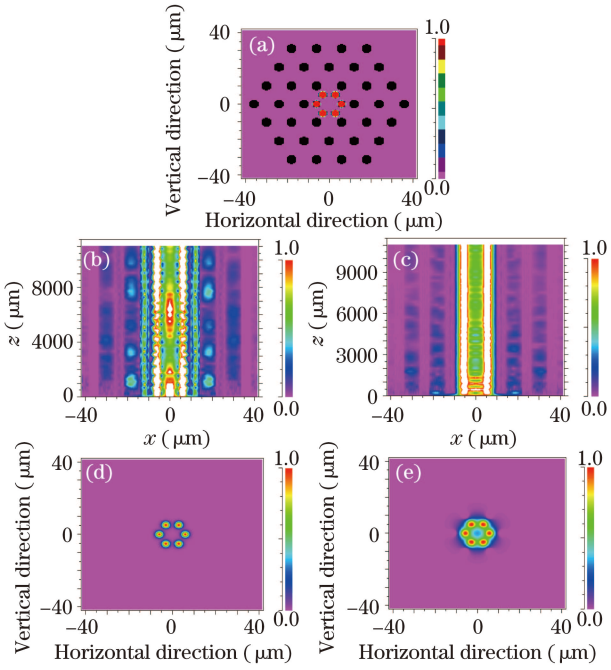

Fig. 2. Characteristics of FEPCFs and propagation of light. (a) Structure of the FEPCF of $d = 4.4$ μm; (b) light propagation at 0.65 μm; (c) light propagation at 1.60 μm; (d) ring mode, $\lambda = 0.65$ μm, $n_{\text{eff}} = 1.470307$; (e) ring mode, $\lambda = 1.60$ μm, $n_{\text{eff}} = 1.449151$.

cores is 4 μm and the pitch of them is 6 μm. The light propagation along the FEPCF clearly differs from that along the ESPCF. In addition, the propagation of light is relative to the wavelength. At the short wavelength (Fig. 2(b)), e.g., $\lambda = 0.65$ μm, the energy oscillates between two modes periodically. On the other side, the central injected mode could convert to ring mode at long wavelength (Fig. 2(c)). Using simulation software developed by CUDOS group[12], we obtain the mode fields at different wavelengths, as shown in Figs. 2(d) and (e). The simulation result shows that the high-index cores concentrate more energy inside them at shorter wavelength, while the mode field spreads in more area at longer wavelength.

We simulate the light propagation along FEPCF at different wavelengths by changing the air-hole diameter in the cladding or the pitch or diameter of embedded cores. The injected mode is always Gaussian and the pitch of cladding holes is fixed at 12 μm. After comparing the simulation results, we propose some optimized structures to make mode converters from Gaussian to annular.

To find the optimized structure to make a mode converter at different wavelengths, we chose different parameters of the FEPCF, including the diameter of the air holes and embedded cores and the pitch between them. We study them individually below.

First of all, we changed the cladding air hole from 4.4 to 7.6 μm (Fig. 3(a)). By comparing the mode fields of FEPCF of 7.6-μm air holes (Figs. 3(b) and (c)) with that of 4.4-μm air holes (Figs. 2(b) and (c)) at 0.65 and 1.60 μm, we find that the FEPCF air-hole pitch of 4.4 μm has better mode transferring effect, i.e., it transfers more energy from the Gaussian mode to the ring mode in a short propagation length at 1.60 μm.

We also analyze the effect of the diameter d_{core} of the embedded high-index cores. Decreasing d_{core} from 4 to 3 μm and keeping other parameters the same as those in Fig. 2 (Fig. 4(a)), the light propagation at 1.60 μm has clear beating phenomenon (Figs. 4(b) and (c)).

Then we change the pitch of the embedded cores Λ_{core} from 6 to 4.08 μm (Fig. 5(a)). The simulation shows that

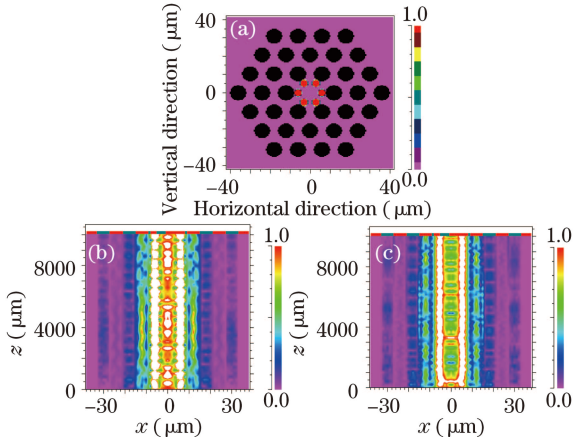

Fig. 3. Effect of the embedded PCFs with inflated air holes. (a) Structure of the FEPCF of $d = 7.6$ μm; (b) light propagation at 0.65 μm; (c) light propagation at 1.60 μm.

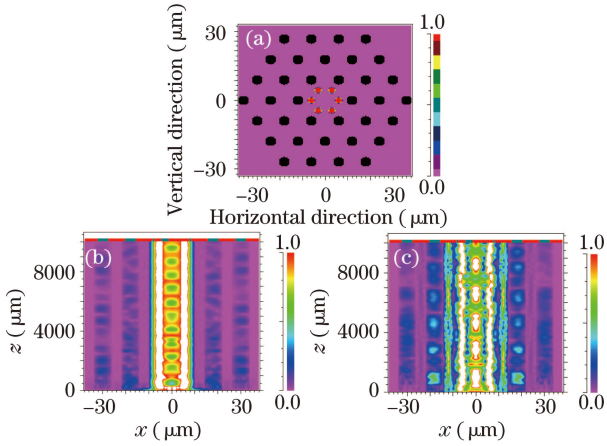

Fig. 4. Effect of the embedded PCFs with smaller embedded cores. (a) Diameter of the embedded core is $d = 3$ μm; (b) light propagation at 0.65 μm; (c) light propagation at 1.60 μm.

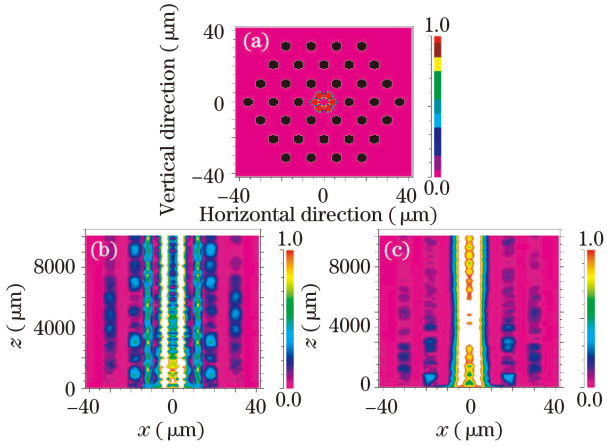

Fig. 5. Effect of the embedded PCFs with pitch of embedded cores being 4.08 μm. (a) FEPCF structure; (b) light propagation at 0.65 μm; (c) light propagation at 1.60 μm.

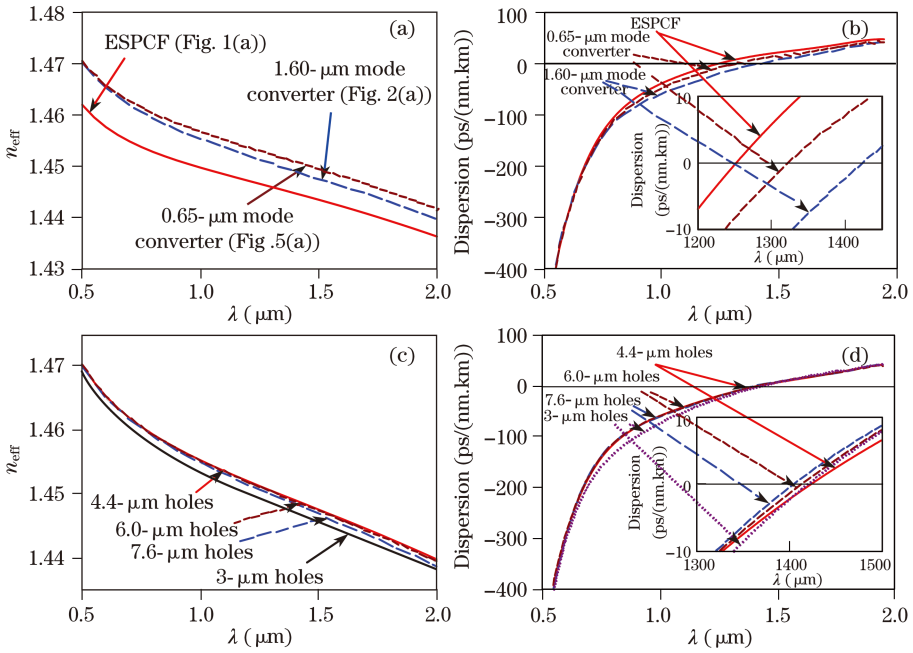

Fig. 6. Effective refractive indices and dispersion curves of different PCFs. (a) Effective refractive indices of different PCFs; (b) dispersion curves of different PCFs; (c) effective refractive indices of different FEPCFs; (d) dispersion curves of different FEPCFs.

FEPCF with the pitch of 4.08 μm transfers more light to the ring mode at 0.65 μm (Fig. 5(b)). For the long wavelength of 1.60 μm, the light is confined in the central area (Fig. 5(c)).

Based on the simulation results, we choose two optimized mode converters for short and long wavelengths. To make a mode converter at short wavelength, we prefer the FEPCF as shown in Fig. 5(a), for which the embedded cores are 4 μm in diameter and 4.08 μm in pitch, and the cladding air holes are 4.4 μm in diameter and 12 μm in pitch. For the long wavelength, the structure of 6-μm pitch shown in Fig. 2(a) is a better choice.

To analyze the dispersion characteristics of the FEPCF, we calculate the effective refractive index $n_{\rm eff}$ at different wavelengths for different structures of PCF. Then we calculate the dispersion curve based on

$$D = -\frac{\lambda}{c}\frac{{\rm d}^2{\rm Re}(n_{\rm eff})}{{\rm d}\lambda^2} \quad (1)$$

for different situations, and find the zero-dispersion wavelength for different structures, as shown in Fig. 6(a). In Eq. (1), D is the dispersion, λ is the wavelength, and c is the light speed in vacuum.

The zero-dispersion wavelength for ESPCF shown in Fig. 1(a) is about 1.25 μm. After embedding the high-index cores (Fig. 2(a)), the zero-dispersion wavelength shifts to 1.42 μm (Fig. 6(b)). For the optimized converter structure at short wavelength, the zero-dispersion wavelength is around 1.32 μm.

At last, we change the diameter of cladding air holes from 4.4 to 7.6 μm and calculate the effective index and the dispersion curve, while the embedded core diameter is kept at 4 μm. A curve representing the structure of 3-μm embedded core shown in Fig. 4(a) is added for comparison. The results show that the zero-dispersion wavelengths are almost the same (Figs. 6(c) and (d)).

In conclusion, we design several kinds of FEPCFs and analyze their characteristics. FEPCF can convert a Gaussian mode to a ring mode as a mode converter. We calculate the mode fields, the effective refractive indices, and dispersion curves for wavelengths from 0.5 to 2.0 μm in different FEPCF structures. Two optimized mode converters are designed and analyzed at wavelengths of 1.60 and 0.65 μm. The FEPCF-based mode converter can be easily produced and applied, and it is a better choice for commercial converters.

This work was suopported by the Heilongjiang Grant for Young Leading Teachers (No. 1151G071) and the Harbin Technology Foundation for Oversee Returnee (No. 2007RFLXG007).

References

1. J. C. Knight, T. A. Birks, P. St. J. Russell, and D. M. Atkin, Opt. Lett. **21,** 1547 (1996).
2. J. C. Knight, Nature **424,** 847 (2003).
3. K. Lai, S. G. Leon-Saval, A. Witkowska, W. J. Wadsworth, and T. A. Birks, Opt. Lett. **32,** 328 (2007).
4. C. D. Poole, J. M. Wiesenfeld, D. J. DiGiovanni, and A. M. Vengsarkar, J. Lightwave Technol. **12,** 1746 (1994).
5. C. D. Poole, J. M. Wiesenfeld, A. R. McCormick, and K. T. Nelson, Opt. Lett. **17,** 985 (1992).
6. S. G. Johnson, M. Ibanescu, M. Skorobogatiy, O. Weisberg, T. D. Engeness, M. Soljačić, S. A. Jacobs, J. D. Joannopoulos, and Y. Fink, Opt. Express **9,** 748 (2001).
7. S. Choi and K. Oh, Opt. Commun. **221,** 307 (2003).
8. A. Witkowska, S. G. Leon-Saval, A. Pham, and T. A. Birks, Opt. Lett. **33,** 306 (2008).
9. W. Sun, X. Liu, F. Fu, and J. Zhang, Chin. Opt. Lett. **6,** 715 (2008).
10. T. A. Birks, J. C. Knight, and P. St. J. Russell, Opt. Lett. **22,** 961 (1997).
11. W. Chen, J. Li, S. Li, H. Li, Z. Jiang, and J. Peng, Chin. Opt. Lett. **5,** 383 (2007).
12. T. P. White, B. T. Kuhlmey, R. C. McPhedran, D. Maystre, G. Renversez, C. M. de Strerke, and L. C. Botten, J. Opt. Soc. Am. B **19,** 2322 (2002).